



Nanosensing of ATP by fluorescence recovery after surface energy transfer between rhodamine B and curcubit[7]uril-capped gold nanoparticles

Riham El Kurdi¹ · Digambara Patra¹

Received: 8 May 2018 / Accepted: 28 June 2018 / Published online: 2 July 2018
© Springer-Verlag GmbH Austria, part of Springer Nature 2018

Abstract

The authors describe a method for functionalization of gold nanoparticles (AuNPs) with the supramolecular host molecule, curcubit[7]uril (CB[7]) which can bind rhodamine B (RhB). The fluorescence of RhB is quenched by the AuNPs via surface energy transfer. On addition of ATP, a dimeric RhB-ATP complex is formed and RhB is pushed out of CB[7]. Hence, fluorescence increases by a factor of 8. This fluorescence recovery effect has been utilized to develop a new detection scheme for ATP. The assay, measured at fluorescence excitation and emission wavelengths of 500 nm and 574 nm respectively, works in the 0.5–10 μM concentration range and has a 100 nM detection limit. The method is not interfered by UTP, GTP, CTP, TTP, ascorbic acid and glutathione.

Keywords AuNPs · ATP · Curcubit[7]uril · Surface energy transfer · Fluorescence · Rhodamine B · Nanosensing · Supramolecular functionalization

Introduction

Gold nanoparticles (AuNPs) in several shapes are synthesized using chemical, physical and biological methods [1]. At a specific wavelength of light, collective oscillation of electrons on the AuNPs surface cause a phenomenon called surface plasmon resonance, resulting in strong extinction of light as scattering and absorption [2]. This absorption is useful for developing various analytical applications. Moreover, use of AuNPs requires complex modifications or alteration on their surfaces with regard to accomplish the desired efficacy and limit off target toxicity. Particularly, the use of AuNPs in biological settings claims their previous functionalization with one or several biomolecules such as DNA/RNA, oligonucleotides, peptides and antibodies. In addition, fluorescent dyes,

polymers, drugs, tumor markers, enzymes and other proteins can be introduced to the required functionalities [3]. Surface modification of AuNPs present several advantages, such as, (a) it increases circulation lifetime of conjugates by preventing or slowing their removal, (b) it helps in attaching molecules specifically to locate and attach to targeted cells, (c) it can improve stability, and (d) it can reduce non-specific cytotoxicity by capping AuNPs.

In addition to the applications in optoelectronics and biomedicine, gold nanoparticles are well-known to have a superior fluorescence quenching efficiency in a wide range of wavelengths compared to the organic quenchers fascinating new possibilities for exploring surface energy transfer (SET) phenomena [4–6]. In this case, energy transfer occurs from a donor molecule to a nanoparticle surface at a much slower decay rate than the dipole-dipole energy transfer in FRET [4, 7]. SET from dye molecule to the AuNPs follows $1/d^4$ distance dependence [6]. Further, AuNPs have unique size dependent SPR, their absorption band can be tuned easily and precisely by changing its shape and size in such a way that their absorption band overlaps with fluorescence band of a chosen fluorophore. This situation is considered an efficient transfer of energy from the excited fluorophore to the gold nanoparticle surface leading to the

Electronic supplementary material The online version of this article (<https://doi.org/10.1007/s00604-018-2901-8>) contains supplementary material, which is available to authorized users.

✉ Digambara Patra
dp03@aub.edu.lb

¹ Department of Chemistry, American University of Beirut, PO Box 11-0236, Riad El Solh, Beirut 1107 2020, Lebanon

reduction of the fluorescence [8]. As an example of dyes, rhodamine is considered as one of important dyes. Sen et al. have also successfully established SET from rhodamine 6G to AuNPs [6].

It has been demonstrated that supramolecular encapsulation of fluorescent molecules, such as rhodamines, by macrocyclic host molecule like cucurbit[n]uril (CB[n]) can improve their fluorescence properties and photochemical stability due to an altered microenvironment [9]. Encapsulation of fluorescence dyes by CBs enhances the fluorescence intensity preventing the dimer aggregation of dyes, providing the dyes fit into cavity of the host, accessed through their carbonyl-lined portals [10]. In general, cucurbit[n]urils are hollow barrel-shaped macrocyclic molecules having a pair of hydrophilic carbonyl portals at both ends and a hydrophobic cavity inside. This results in the ability of CBs to bind a wide range of neutral and cationic guests in aqueous solutions by non-covalent supramolecular interactions [10]. Cucurbit[7]uril (CB[7]) has substantially higher solubility in water than CB[6] and CB[8], larger voluminous cavity than its water soluble analogue CB[5] and thus has been used to form strong and stable inclusion complexes with fluorescent rhodamine [11].

Adenosine Triphosphate (ATP) plays a significant role in cellular energetics, metabolic regulation and cellular signaling and therefore many different methods have been developed to detect ATP molecules, including colorimetric methods using gold nanoparticles as probes and metal ions as cross-linkers [12, 13]. Aptamer are getting popular due to its increase specificity. Wang et al. have developed a detection method using gold nanoparticles-based aptamer for ATP assay [14]. Other methods were based on electrochemical sensing [15] and fluorescence probing [16, 17]. There are various other methods reported for ATP estimation using aptamer [18–24]. Pu et al. have developed a graphene oxide base on aptamer chemistry to detect ATP [18]. Similarly, Qiu et al. have reported aptamer based turn-off fluorescent ATP assay using DNA concatamers [19]. Cheng et al. have established an ATP assay applying aptamer based fluorometric determination of ATP by exploiting the FRET between carbon dots and graphene oxide [24]. Fluorescence based method has drawn interest because of its sensitivity [20, 21, 23]. Similarly, many different kinds of nanomaterials are employed as fluorescence quencher to develop scheme for the determination of ATP. In this study, CB [7] capped and stabilized AuNP/AuNRs have been used as host molecule to form inclusion complex with rhodamine B (as guest) as a result of which SET occurs between RhB and CB[7] capped AuNPs by diminishing fluorescence intensity of RhB. Addition of ATP selectively recovers this lost fluorescence of RhB and this fluorescence recovery has been utilized to design a new sensing system for ATP.

Materials and methods

Materials

Curcumin and cucurbit[7]uril were obtained from Sigma Aldrich (<https://www.sigmaaldrich.com/european-export.html>). Adenosine 5'-Triphosphate disodium salt and gold (III) chloride were purchased from Acros (<https://www.acros.com>). Uridine 5'-Triphosphate disodium salt, Cytidine 5'-Triphosphate disodium salt (CTP), Thymidine 5'-Triphosphate disodium salt (TTP), Guanosine 5'-Triphosphate disodium salt (GTP), ascorbic acid, and glutathione were obtained from Sigma (<https://www.sigmaaldrich.com/european-export.html>). All the chemicals were used without further purification and dissolved in double distilled water except that stock of curcumin was prepared in methanol. Detailed characterization and spectroscopic measurements has been given Electronic Supplementary Material.

Synthesis of stabilized cucurbit[7]uril gold nanoparticles/rods

The synthesis was carried out in basic aqueous media since cucurbit[7]uril is insoluble in double distilled water (DDW). 1 mL of 50 μM of CB[7] prepared in basic media was dissolved in 14 mL of DDW and left for 15 min at 45 $^{\circ}\text{C}$. To this solution, 15 mL of 1 mM of HAuCl_4 prepared in DDW was added. Then 1 mL of 10 mM of curcumin prepared in methanol was mixed to have a final volume of 31 mL and the solution was stirred at 400 rpm for 2 min. Finally, the solution was kept at 45 $^{\circ}\text{C}$ for 24 h. To precipitate the gold, the final solution was centrifuged at 37800 \times g for 25 min.

Sample for rhodamine and adenosine triphosphate detection

AuNPs were dissolved in 10 mL double distilled water. From this AuNPs stock, 0.1 mL of solution was taken for the assay. Separately, 50 μM of ATP stock solution was prepared in DDW and different volumes of ATP solution was added to the 0.1 mL AuNPs solution to prepare separately different concentrations of ATP in the range of 0 to 10 μM . Similarly, 50 μM stock solution of rhodamine B was prepared in DDW and a given volume of rhodamine B solution was added to AuNPs solution to have 5 μM of rhodamine B concentration in the final solution with a final volume of 3 mL. Interference study was carried out similarly by preparing 50 μM stock solution of CTP, UTP, GTP, TTP, ascorbic acid, glutathione etc. separately and adding a known volume of this solution to keep the final concentration, ~ 10 μM in the final solution. For

calibration curve, fluorescence intensity was measured at excitation and emission wavelengths 500 nm and 574 nm respectively.

Results and discussion

The cucurbit[7]uril-stabilized gold nanoparticles/nanorods were synthesized using curcumin as reducing agent [25, 26]. These particles were monitored by Resonance Rayleigh Scattering (RRS) and UV-Visible absorbance spectra. As shown in Fig. 1a, AuNP/AuNRs gave two major RRS peaks at ~435 nm and at ~550 nm and a minor peak at ~380 nm. Similarly, the absorption maximum of AuNP/AuNRs was found to be at ~610 nm (see Fig. 1b). The concentration of the prepared AuNP/AuNRs was calculated based on Lambert-Beer's law:

$$A = l \times C \times \epsilon$$

To evaluate definite value for the extinction coefficient (ϵ) of AuNP/AuNRs at 600 nm, ϵ was estimated to be 1.03×10^9 according to the below equation [27].

$$\ln \epsilon = k \ln D + a$$

where D is the core diameter of the AuNPs, $k = 3.32111$ and $a = 10.80505$.

From this equation, the molar concentration of the AuNPs was calculated to be 0.145 nM. The prepared AuNP/AuNRs were characterized by scanning electron microscopy to evaluate the morphology and sizes of AuNPs. As noticed in Figure S1A&B (Electronic Supplementary Information), the synthesized AuNPs were present in two different shapes; they are

present in a good spherical shape with 20–30 nm diameters, in addition to the formation of rods shape. The particles formed were negatively charged and that was verified by zeta potential analysis where the value was equal to -23.63 mV (see Figure S1C).

Gold nanoparticles, with a diameter between 1 nm and 100 nm, have been extensively used in chemical and biological sensors because of their excellent physical and chemical properties. In this case, rhodamine b was used as a fluorescent dye owing to its high fluorescence quantum yield, high extinction coefficient and good photostability. The UV-Vis absorption of RhB in water is depicted in Fig. 2a. The absorption curve of RhB showed a strong absorption band at 556 nm, characteristic to π - π^* electronic transition monomers and a weak band at 520 nm assigned to the dimeric states of RhB molecules. It is known that in aqueous solution, the monomers are in equilibrium with dimers and the molar fraction of the dimers varies with RhB concentration [28]. The fluorescence of RhB molecules in the presence of different volume of AuNPs was evaluated. In fact, RhB molecules in solution are positively charged so they can adsorb onto the surface of the negatively charged AuNP/AuNRs through electrostatic interactions and can resist van der Waals attraction. Moreover, this interaction is further facilitated by cucurbit[7]uril as a host molecule for RhB at the surface of AuNPs. Thus, fluorescence intensity of RhB was greatly reduced by AuNP/AuNRs, this processes between them suggests that SET is taking place with AuNP/AuNRs as acceptor and RhB as donor [6]. This was further reestablished by overlapping of emission spectrum of rhodamine b and absorption spectrum of AuNPs as depicted in Fig. 2b. Thus, if RhB and AuNP/AuNRs coexist together in a such system, the fluorescence intensity of RhB should diminish. This hypothesis was confirmed because the fluorescence intensity of RhB

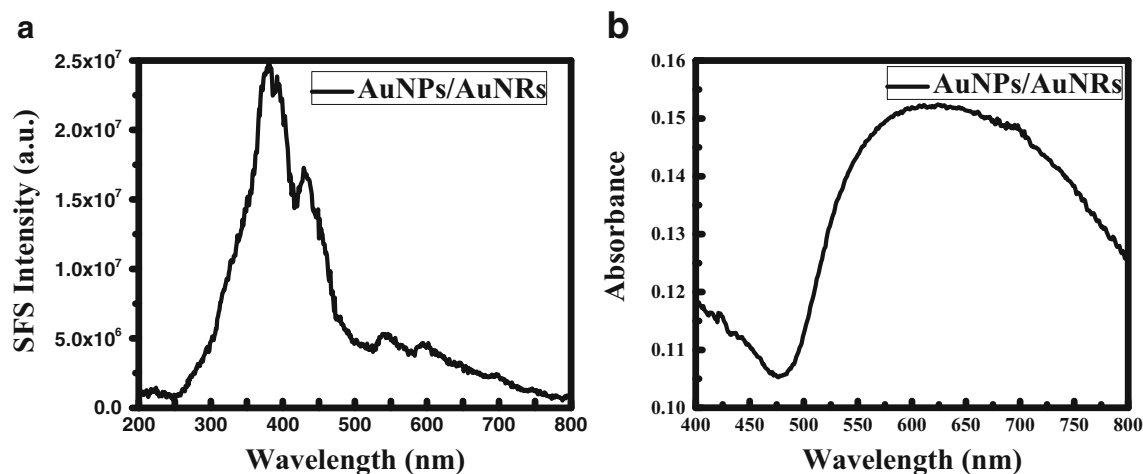


Fig. 1 Synchronous fluorescence spectra at $\Delta\lambda = 0$ nm (a) UV-Vis spectra (b) and of cucurbit [7] uril and curcumin functionalized Au nanoparticles/nanorods

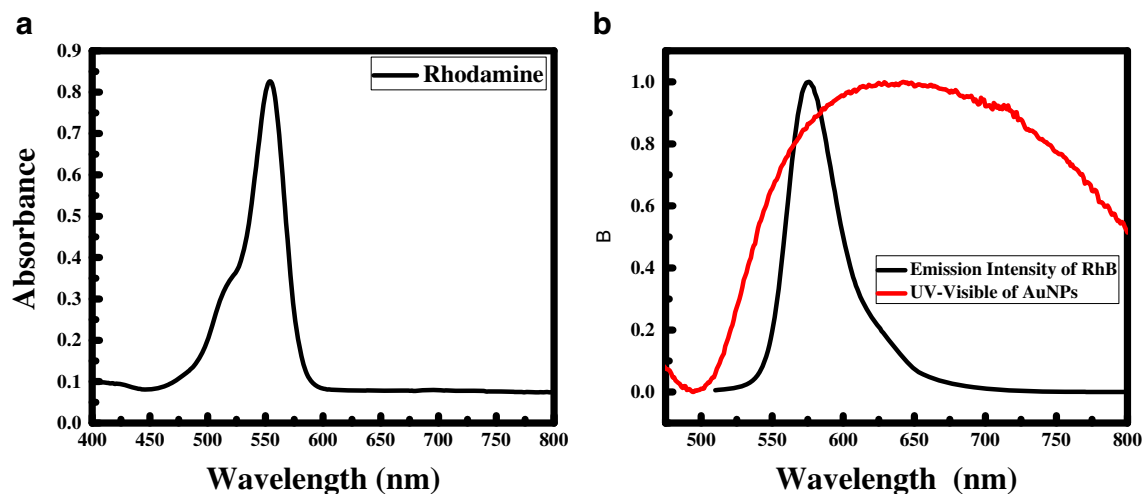


Fig. 2 **a** UV-Vis spectra for Rhodamine b in water; **(b)** overlapping of emission spectrum of rhodamine b and absorption spectrum of AuNPs

consistently decreased upon the addition of AuNP/AuNRs, as seen in Fig. 3a. For the reduction in fluorescence, the quenching efficiency can be defined as $(I_0 - I)/I_0$ where I_0 and I respectively represent the fluorescence intensity of RhB in the absence and presence of AuNP/AuNRs. Thus, the quenching constant (K_{sv}) can be calculated based on Stern-Volmer equation:

$$I_0/I = K_{sv} \times C_{AuNPs} + 1$$

The plot between I_0/I and the concentration of AuNPs is shown in Fig. 3b, where a good linear relationship (with $R^2 = 0.996$) was obtained in a wide concentration range and the Stern - Volmer equation can be fitted as:

$$I_0/I = 0.734 \times C_{AuNPs} + 1$$

Where the K_{sv} was calculated to be $0.734 \times 10^9 \text{ M}^{-1}$. Thereby, K_{sv} is considered as large verifying that the AuNP/AuNRs

capped with CB[7] are excellent as acceptor for RhB, which acts as the donor during SET. The excited state life time of RhB in water was measured and found to be 1.74 ns [29], so the biomolecular quenching rate constant was estimated to be $4.21 \times 10^{17} \text{ M}^{-1} \text{ s}^{-1}$, according to the following equation:

$$K_{sv} = k_d \times \tau_0$$

This suggests the quenching rate is diffusion controlled. The quantum efficiency of fluorescence for rhodamine was estimated to be relatively high. Defining the $\phi_0 = 0.31$ [30] after the determination of unperturbed RhB in water, the quantum efficiency of dye RhB fluorescence is calculated as follow:

$$\phi_q = \phi_0 k (I/I_0)$$

where I and I_0 are the fluorescence intensity for RhB respectively in presence and absence of AuNPs, and k is the correction factor for chemical quenching, means formation of

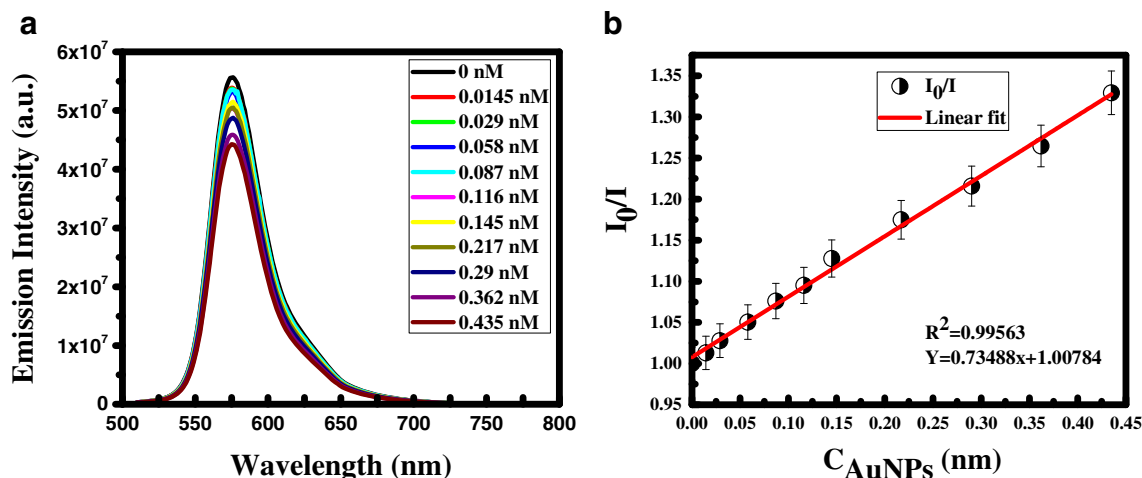


Fig. 3 **a** Emission spectrum excited at $\lambda = 500 \text{ nm}$ of Rhodamine B with different concentration of cucurbit[7]uril and curcumin functionalized AuNP/AuNRs; **(b)** Linear correlation of I_0/I emission intensity of Rhodamine b vs. concentration AuNP/AuNRs. For all the measurements, $n = 3$

dimers. The value of obtained ϕ_q was 0.044, which confirms the quenching effectiveness of fluorescence of RhB by AuNP/AuNRs. This value is also in the range of quantum efficiency calculated by Daniela et al. where ϕ_q was found to be between 0.01 and 0.045 [31].

While increasing the concentration of RhB from 0 to 10 μM and fixing the concentration of AuNPs, an enhancement of the fluorescence emission intensity, best measured at excitation and emission wavelengths 500 and 574 nm, was observed (see Figure S2A, Electronic Supplementary Material). From the plot of fluorescence intensity vs. the concentration of RhB (see Figure S2B; Electronic Supplementary Material), it was seen that the fluorescence intensity is linear up to 5 μM and then it showed a little negative deviation from the linearity. The negative deviation can be due to chemical effect such as H-aggregate formation [32], which is possible when enough RhB are present in the solution compared to number of curcubit[7]uril at the surface of AuNPs. The I/I_0 plot vs. the concentration of RhB is plotted in Figure S2C,

where the curve showed linear change. This linear increase was fitted with a linear equation, $Y = 282.45x + 187.7$ with $R^2 = 0.99$.

Gold nanoparticles, nanorods, nanowires have been applied to detect DNA, metal ions and other small molecules using fluorescence emission intensity [25, 26]. Hence, the prepared AuNP/AuNRs linked to RhB were used to detect ATP molecule. In fact, the ring nitrogen of hybrid aromatics and primary amines with electron-rich nitrogen atoms are more plausibly to get attached onto the surface of metal nanoparticles through the coordinating interactions with the electron-deficient surface of metal nanoparticles [12]. In addition, ATP possesses multiple binding sites, consisting of one exocyclic amino group and/or two double nitrogen hybrid rings, which can strongly coordinate to AuNP/AuNRs by ligand exchange [33]. The ability of AuNP/AuNRs to detect ATP in the presence of RhB was established by measuring the fluorescence emission intensity while increasing the concentration of ATP (see Fig. 4a). RhB forms dimeric RhB-ATP complexes

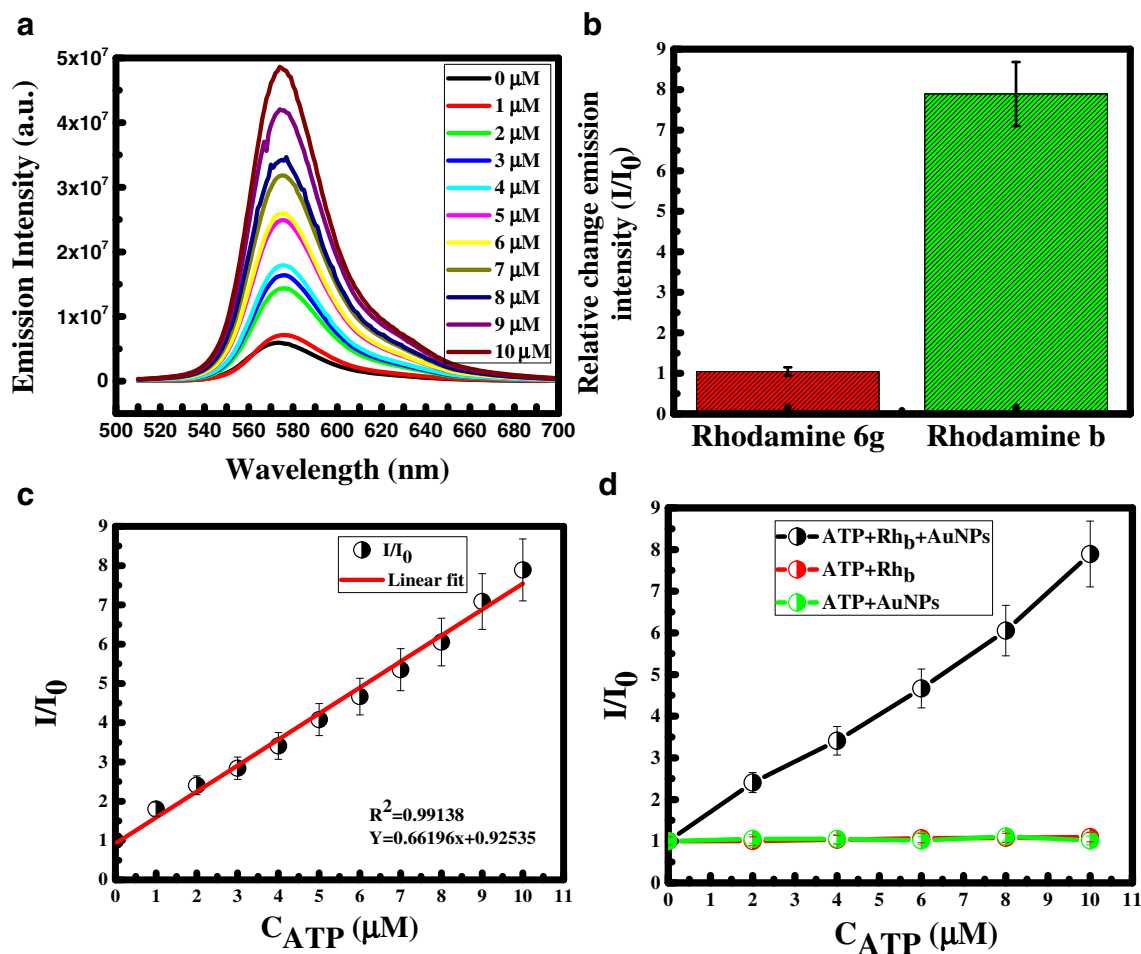


Fig. 4 a Emission spectrum excited at $\lambda = 500$ nm of AuNP/AuNRs-Rhodamine b system with different concentration of ATP; (b) Ratio of emission intensity (I/I_0) of AuNP/AuNRs with Rhodamine b and Rhodamine 6g; (c) Linear correlation of I/I_0 emission intensity of AuNP/AuNRs-Rhodamine B system vs. concentration ATP; (d) I/I_0

For ATP detection with AuNP/AuNRs-Rhodamine b system, Rhodamine B alone and AuNP/AuNRs alone. Emission intensity (I) was collected at excitation and emission wavelengths 500 nm and 574 nm, respectively. For all the measurements, $n = 3$

by coordinating to the triphosphate groups and adenine ring nitrogen. It is obvious that interaction of AuNPs with ATP pushes RhB away from AuNPs increasing the distance between RhB and AuNPs, which reduces the SET efficiency and recovers the lost fluorescence (due to SET as reported earlier [6]). In this case such recovery of fluorescence after SET enhanced the fluorescence intensity about ~8 fold. Furthermore, to understand that whether slight change in structure of probe molecule has any role during estimation of ATP, the probe molecule was changed to rhodamine 6G instead of RhB. Interestingly, as it is presented in Fig. 4b, the fluorescence recovery did not show significant improvement by using rhodamine 6G compared to ~8 fold enhancement while using RhB. It is reported that association constant of rhodamine 6G with curcubit[7]uril is ~7 fold higher than that of RhB [34], therefore, beside direct interaction between AuNPs and ATP, association of probe (RhB) with curcubit[7]uril plays a significant role.

In case of RhB, the fluorescence emission intensity also showed a continuous recovery with the increase in ATP concentration till 10 μM . For a range of concentration between 0.5 and 10 μM , the corresponding linear regression equation was $Y = 0.662x + 0.925$ with $R^2 = 0.991$ (see Fig. 4c). The detection limit was estimated on the $3\sigma/m$ criterion (where σ is the standard deviation of the blank and m is the slope of the calibration plot. For ATP determination detection limit was found to be 100 nM. This concentration ranges and detection limit is similar to the literature reported value for the determination of ATP using fluorescence-based nanomaterials as summarized in Table 1, though some of the electrochemical methods work in lower concentration ranges [15, 20].

To make sure that there is no specific interaction between RhB and ATP, fluorescence measurement was

carried out for AuNP/AuNRs alone and RhB alone for different concentration of ATP as shown in Fig. 4d. There was no significant change in fluorescence intensity of RhB (in the absence of AuNPs) at different concentration of ATP, similarly fluorescence signal of AuNPs alone was not affected by different concentration of ATP in the absence of RhB suggesting that both AuNPs and RhB are essential for the ATP determination. The analytical recovery of samples using the present method was estimated by testing 3 unknown samples using the above fitted calibration curve obtained. The results obtained are summarized in Table 2. The percent of recovery ATP of our method was found to be between 97 and 101% ± 3.1 ($n = 3$).

The selectivity and the specificity of the AuNP/AuNRs system was evaluated by following the fluorescence emission intensity of the AuNP/AuNRs in presence of other analogs biomolecules such as UTP, GTP, CTP, TTP, ascorbic acid and glutathione due to the fact that they had similar molecule structures (like ATP) and in consequence interferes with the detection in practical applications. The results presented in Fig. 5 indicate that when the concentration of the six analogs increases, only ATP had an obvious recovery of fluorescence intensity and no change in fluorescence signal of RhB-AuNPs system was observed in the presence of either UTP, GTP, CTP, TTP, ascorbic acid or glutathione. This excellent selectivity can be primarily attributable to the binding property of triphosphate groups of ATP with RhB and the high adsorption of adenine onto the surface of the AuNPs. Similar results have been reported by Meng et al. [35] where they have designed aptamer sensors to detect ATP and by Deng et al. [12] using gold nanoparticles with metal ions cross-linkers for the detection of ATP.

Table 1 An overview on recently reported nanomaterial-based methods for determination of ATP

Methods	Concentration Range	Selectivity towards Analogues	LOD	References
Gold nanoparticles as colorimetric probes and metal ions as cross-linkers	2–12 μM	UTP, GTP, CTP	50 nM	[12]
Gold particle colorimetric aptamer	4.4–132.7 μM	Not reported	2.0 μM	[14]
DNAzyme-amplified electrochemical detection	0.1–1000 nM	UTP, GTP, CTP	50 pM	[15]
Oxytetracycline (OTC)– Eu^{3+} as a fluorescence probe	80 nM –1.5 μM	Metal ions and amino acids	2.67 nM	[16]
Norfloxacin– Tb^{3+} as a fluorescence probe	1–16 μM	Metal ions and amino acids	41.3 nM	[17]
Graphene oxide based fluorescence aptamer	3–320 μM	UTP, GTP, CTP	450 nM	[18]
DNA concatamers	7–5000 μM	ADP, dNTP, phosphates	6.1 μM	[19]
Fluorometric based on deoxyribonuclease I-aided using graphene oxide as a quencher	10–400 nM	UTP, GTP, CTP	0.2 nM	[20]
Target-cycling strand displacement amplification and copper nanoclusters	0.01–100 nM	UTP, GTP, CTP	5 pM	[21]
Colorimetric and visual determination using boronic acid	8–100 μM	UTP, GTP, CTP	0.12 μM	[22]
Labeled aptamer and magnetic nanoparticles	0.1–100 μM	UTP, GTP, CTP	89 nM	[23]
FRET between carbon dots and graphene oxide	0.1–5 nM	UTP, GTP, CTP	80 pM	[24]
FRET between Rhodamine b and AuNPs	0.5–10 μM	UTP, GTP, CTP	100 nM	This work

Table 2 Recovery results of the proposed method

	Theoretical concentration ($\mu\text{mol}\cdot\text{L}^{-1}$)	Experimental concentration ($\mu\text{mol}\cdot\text{L}^{-1}$)	Recovery (%)
Unknown 1	1	0.971	97
Unknown 2	4	4.023	101
Unknown 3	8	7.875	98

Data were obtained using standard addition method

Conclusion

Functionalization of AuNP/AuNRs with a supramolecular host molecule, CB[7], was successfully achieved, which can be exploited for the development of analytical methods for biomedical application. It was found that CB[7] facilitates to bring RhB near to the AuNPs for effectively resulting SET between RhB and AuNPs. The rate of reduction in fluorescence was remarkable with a biomolecular quenching rate constant of $\sim 10^{17} \text{ M}^{-1} \text{ s}^{-1}$ suggesting the process is diffusion controlled. Obtained ϕ_q value established the SET effectiveness of fluorescence of RhB by CB[7] capped AuNPs/AuNRs. In the presence of ATP, RhB formed dimeric RhB-ATP complexes by coordinating to the triphosphate groups and adenine ring nitrogen recovering the fluorescence intensity to ~ 8 fold. Interestingly, strong association between rhodamine 6 g (having similar structure like RhB) and CB [7] did not help to recover this fluorescence as expected, thus, relatively weak association of RhB with CB[7] plays a role in recovering lost fluorescence by ATP. Fluorescence recovery

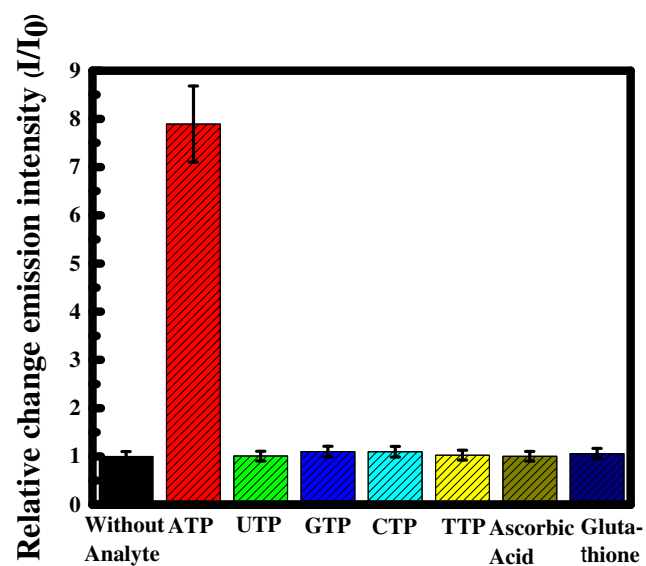


Fig. 5 Ratio of emission intensity (I/I_0) of AuNP/AuNRs-Rhodamine b in the presence of ATP, UTP, GTP, CTP, TTP, ascorbic acid and glutathione. For all the measurements, $n = 3$

of RhB after SET was used to develop a new nanosensing scheme for the estimation of ATP in the concentration found in literature [12, 14, 17, 22, 23]. However, this method does not work in very low concentration range ($< 100 \text{ nM}$) reported using electrochemical methods [15, 20] and sensitivity needs to be further improved to 0.1 nM for commercially available luciferase assay. Though presence of other similar biological analogs biomolecules such as UTP, GTP, CTP, TTP, ascorbic acid etc. did not interfere during ATP determination, a detailed study on field samples will enhance applicability of the present method.

Acknowledgements Financial support provided by Lebanese National Council of Scientific Research (NCSR), Lebanon and American University of Beirut, Lebanon through URB, K. Shair CRSL endowed research fund as well as Kamal A. Shair Central Research Laboratory (KAS CRSL) facilities to carry out this work is greatly acknowledged.

Compliance with ethical standards The author(s) declare that they have no competing interests.

References

- Sharma N, Bhatt G, Kothiyal P (2015) Gold nanoparticles synthesis, properties, and forthcoming applications – a review. *Indian J Pharm Biol Res* 3(2):13–27
- El-sayed IH, Huang X, El-sayed MA (2005) Surface Plasmon resonance scattering and absorption of anti-EGFR antibody conjugated gold nanoparticles in Cancer diagnostics : applications in oral Cancer. *Nano Lett* 5(5):829–834
- Cai W, Gao T, Hong H, Sun J (2008) Applications of gold nanoparticles in cancer nanotechnology. *Nanotechnol Sci Appl* 32:17–32
- Zu F, Yan F, Bai Z, Xu J, Wang Y, Huang Y, Zhou X (2017) The quenching of the fluorescence of carbon dots: a review on mechanisms and applications. *Microchim Acta* 184:1899–1914
- Chen Y, O'Donoghue MB, Huang Y-F, Kang H, Phillips JA, Chen X, Estevez M-C, Yang CJ, Tan W (2010) A surface energy transfer nanoruler for measuring binding site distances on live cell surfaces. *J Am Chem Soc* 132:16559–16570
- Sen T, Sadhu S, Patra A (2007) Surface energy transfer from rhodamine 6G to gold nanoparticles: a spectroscopic rules. *Appl Phys Lett* 91:043104
- Chance R, Prock A, Silbey R (1978) Molecular fluorescence and energy transfer near interfaces. *Adv Chem Phys* 60:1
- Ghosh D, Chattopadhyay N (2013) Gold nanoparticles : acceptors for efficient energy transfer from the Photoexcited fluorophores. *Opt Photonics J* 3:18–26
- Gupta M, Maity DK, Singh MK, Nayak SK, Ray AK (2012) Supramolecular interaction of coumarin 1 dye with cucurbit[7]uril as host: combined experimental and theoretical study. *J Phys Chem B* 116(18):5551–5558
- Prakash R, Usha G, Piramuthu L, Selvapalam N (2017) Facile detection of cucurbit[7]uril by rhodamine B-decorated nanoparticles. *Chem Soc Jpn* 46:1300–1303
- Heupel M, Gregor I, Becker S, Thiel ER (1999) Photophysical and photochemical properties of electronically excited fluorescent dyes: a new type of time-resolved laser-scanning spectroscopy. *Int J Photoenergy* 1(3):223–229

12. Deng D, Xia N, Li S et al (2012) Simple, fast and selective detection of adenosine triphosphate at physiological pH using unmodified gold nanoparticles as colorimetric probes and metal ions as cross-linkers. *Sensors* 12(11):15078–15087
13. Ishida A, Yamada Y, Kamidate T (2008) Colorimetric method for enzymatic screening assay of ATP using Fe(III)-xylnol orange complex formation. *Anal Bioanal Chem* 392(5):987–994
14. Wang J, Wang L, Liu X, Liang Z, Song S, Li W, Li G, Fan C (2007) A gold nanoparticle-based aptamer target binding readout for ATP assay. *Adv Mater* 19(22):3943–3946
15. Lu L, Si JC, Gao ZF, Zhang Y, Lei JL, Luo HQ, Li NB (2015) Highly selective and sensitive electrochemical biosensor for ATP based on the dual strategy integrating the cofactor-dependent enzymatic ligation reaction with self-cleaving DNAzyme-amplified electrochemical detection. *Biosens Bioelectron* 63:14–20
16. Hou F, Mia Y, Jiang C (2005) Determination of adenosine triphosphate (ATP) using oxytetracycline-Eu³⁺ as a fluorescence probe by spectrofluorimetry. *Spectrochim Acta A* 61:2891–2895
17. Miao Y, Liu J, Hou F, Jiang C (2006) Determination of adenosine disodium triphosphate (ATP) using norfloxacin-Tb³⁺ as a fluorescence probe by spectrofluorimetry. *J Lumin* 116:67–72
18. Pu WD, Zhang L, Huang CZ (2012) Graphene oxide as a nano-platform for ATP detection based on aptamer chemistry. *Anal Methods* 4(6):1662
19. Qiu H, Huang Z, Chen M, Cai X, Weng S, Lin X (2015) Aptamer based turn-off fluorescent ATP assay using DNA concatamers. *Microchim Acta* 182(15–16):2387–2393
20. Ning Y, Wei K, Cheng L, Hu J, Xiang Q (2017) Fluorometric aptamer based determination of adenosine triphosphate based on deoxyribonuclease I-aided target recycling and signal amplification using graphene oxide as a quencher. *Microchim Acta* 184:1847–1854
21. Wang YM, Liu JW, Duan LY, Liu SJ, Jiang JH (2017) Aptamer-based fluorometric determination of ATP by using target-cycling strand displacement amplification and copper nanoclusters. *Microchim Acta* 184(10):4183–4188
22. Jiang G, Zhu W, Shen X, Xu L, Li X, Wang R, Liu C, Zhou X (2017) Colorimetric and visual determination of adenosine triphosphate using a boronic acid as the recognition element, and based on the deaggregation of gold nanoparticles. *Microchim Acta* 184(11):4305–4312
23. Liu X, Lin B, Yu Y, Cao Y, Guo M (2018) A multifunctional probe based on the use of labeled aptamer and magnetic nanoparticles for fluorometric determination of adenosine 5'-triphosphate. *Microchim Acta* 185(4):243
24. Cheng X, Cen Y, Xu G, Wei F, Shi M, Xu X, Sohail M, Hu Q (2018) Aptamer based fluorometric determination of ATP by exploiting the FRET between carbon dots and graphene oxide. *Microchim Acta* 185(2):144
25. El Kurdi R, Patra D (2017) Amplification of resonance Rayleigh scattering of gold nanoparticles by tweaking into nanowires: biosensing of α -tocopherol by enhanced resonance Rayleigh scattering of curcumin capped gold nanowires through non-covalent interaction. *Talanta* 168:82–90
26. El Kurdi R, Patra D (2017) The role of OH⁻ in the formation of highly selective gold nanowires at extreme pH: multi-fold enhancement in the rate of the catalytic reduction reaction by gold nanowires. *Phys Chem Chem Phys* 19(7):5077–5090
27. Lim T-C (2011) *Nanosensors: Theory and Applications in Industry, Healthcare and Defense*. CRC Press, Taylor and Francis Group, Boca Raton
28. Loperz Arbeloa I, Ruiz ojeda P (1982) Dimeric states of rhodamine B. *Chem Phys Lett* 87(6):1–5
29. Berezin MY, Achilefu S (2011) Fluorescence lifetime measurements and biological imaging. *Chem Rev* 110(5):2641–2684
30. Magde D, Rojas GE, Seybold PG (1999) Solvent dependence of the fluorescence lifetimes of xanthene dyes. *Photochem Photobiol* 70(5):737–744
31. Tira DS, Focsan M, Ulinici S, Maniu D, Astilean S (2014) Rhodamine B-coated gold nanoparticles as effective “turn-on” fluorescent sensors for detection of zinc II ions in water. *Spectrosc Lett* 47:153–159
32. Stobiecka M, Hepel M (2011) Multimodal coupling of optical transitions and plasmonic oscillations in rhodamine B modified gold nanoparticles. *Phys Chem Chem Phys* 13(3):1131–1139
33. Kim S, Lee NH, Seo SH, Eom MS, Ahn S, Han MS (2010) Selective colorimetric sensor for Hg²⁺ ions using a mixture of thiourea derivatives and gold nanoparticles stabilized with adenosine triphosphate. *Chem Asian J* 5(12):2463–2466
34. Dsouza RN, Pischel U, Nau WM (2011) Fluorescent dyes and their supramolecular host/guest complexes with macrocycles in aqueous solution. *Chem Rev* 111(12):7941–7980
35. Meng C, Dai Z, Guo W, Chu Y, Chen G (2016) Selective and sensitive fluorescence aptamer biosensors of adenosine triphosphate. *Nanomater Nanotechnol* 6(33):1–6